Chapter 6

Enhancement of C_{60} fragmentation by shaped femtosecond laser pulses

Active control of molecular processes on a microscopic scale has been a dream for many chemists and physicists, which until recently, was hindered by ultrafast energy relaxation pathways. Active control means that "the evolution of the prepared state is partially controlled by the free molecular Hamiltonian and partially controlled by external means"[KRG89]. Control of molecular processes can be achieved through the interaction of an electric field with the molecule. The necessary timescale for the direct manipulation of the electronic and nuclear wavepackets is on the sub picosecond timescale. Nearly arbitrary manipulation of the electric field on these timescales has been achieved with the implementation of computer controlled liquid crystal modulators in fs laser systems. This chapter is an introduction and outlook of the possibilities of using temporally shaped electric fields to control C_{60}.

6.1 Introduction : Pulse Shaping

Control of chemical or physical processes using temporally modulated electric fields, e.g. laser-assisted control, offers an exciting opportunity to study the excitation and relaxation of molecules. The basic idea is to control (or steer) the molecule toward a desired state or reaction pathway by temporal modification of the interacting electric field. The final state or product can then be detected in an experiment.

Microscopically, for small systems, this entails controlling the electronic and vibrational wavepacket motion across the potential energy surface. For larger systems, this picture becomes less clear because there are a large number of possible states

and relaxation pathways. Since many of these processes (and other competing relaxation mechanisms) proceed on a femtosecond time scale, active control was not experimentally feasible until recently with the advent of femtosecond laser radiation.

The first"control" experiments were performed in a pump-dump scheme, initially proposed by Tannor and Rice [TRi85]. In these experiments, a pump pulse is used to excite the system by transferring population to the intermediate state, thus creating a wavepacket. The system is allowed to evolve temporally before a time delayed dump pulse transfers the population back to the ground state. The time delay of the dump pulse creates a selectivity or control of the population transfer to a different product state.

Although this scheme primarily monitors the direction in which a molecule relaxes, by choosing the correct separation of pulses, there is a steering toward a particular product. To steer the molecule into a particular channel, more energy should be input at the correct time on the femtosecond timescale, i.e., with multiple pulses. The theoretical efforts for designing such arbitrarily shaped pulses has been termed optimal control theory (OCT). OCT has been developed by Rabitz and coworkers [PDR88] and Tannor, Rice, and Kosloff [KRG89] for the determination of the optimal electric field to drive a reaction in a particular molecule. The basic problem is reduced to solving the molecular Hamiltonian in an external electric field. One of the major limitations is knowledge of the molecular Hamiltonian, which is generally unknown. This implies that the optimal temporal shape of a pulse cannot be precisely calculated.

Experimentally, a solution around this problem came in the modification of the temporal pulse form of the laser through, for example, liquid crystal modulators [Wei00]. This new tool allows for nearly arbitrary computer controlled phase and/or amplitude masks which can be replaced on the millisecond time scale. The ability to rapidly modify the electric field of a bandwidth limited femtosecond laser pulses nearly arbitrarily allows for searching complex potential energy surfaces for optimum yield of particular channels. This is particularly useful for complex systems where exact calculations are not feasible theoretically. One of the seminal papers in the field of control is [JRa92], where use of a genetic algorithm is proposed in connection with optical pulse shaping techniques to "teach" the laser to control molecules. The idea to incorporate this pulse shaper into a feedback loop to optimize a detected fragment channel has introduced a new way to study molecules. The underlying concept is that the change in pulse form causes a change in the overlap with the propagating wavepackets, which will enhance or suppress the measured yield. From the optimal

shape, qualitative information about the molecular system can be inferred and will aid theoretical calculations for a deeper quantitative understanding.

Femtosecond pulse manipulation is presently used for fundamental research as well as industrial applications. This technique has been applied to many systems, such as small molecules [VBK01, BML01], molecular compounds [ABB98, DFG03], liquids [BYW97, WWB99], and in laser ablation of dielectric surfaces [SBT02]. In this chapter, we apply this technique to C_{60}.

6.1.1 Application to C_{60}

C_{60}, with 60 delocalized π-orbitals and 174 vibrational modes, provides a very challenging system to steer specific reaction pathways. The two most general pathways measurable in a gas phase time of flight experiment are ionization and fragmentation.

The selection to optimize fragmentation is motivated by two observations:

1.) The fragmentation pattern is seen to dramatically change as the pulse duration is changed from 30 fs to 5 ps, even if the fluence is kept constant [CHH01].

2.) Fragmentation patterns resulting from time resolved pump-probe measurements shown in Chapter 5 change depending on the time delay between the two pulses, indicating that there is a time dependence on the energy deposition into the system. Furthermore, it is evident from time resolved pump-probe spectroscopy that the most dramatic changes occur on a sub 4 ps time scale, which corresponds to the maximum time window of the pulse shaping device in the present configuration.

Since higher charged fragments are strongly intensity dependent (see Fig. 5.19), C^+_{60-2n} fragments were used for the optimization procedure. The optimal criterion was chosen as the ratio of A to B, where $A = \sum C^+_{60-2n}$ and $B = C^+_{60}$ multiplied by a linear weighting of the signal A within each generation. Since this ratio can be optimized by either maximizing fragmentation yield or minimizing the C^+_{60} yield, a linear weighting was chosen for the fragments so that a higher signal has a better fitness. The linear weighting was achieved by multiplying each individual by A/A_{max}, where A_{max} is the maximum signal of A per generation. Thus the fitness, F, is defined as

$$F = \frac{\sum C^+_{60-2n}}{C^+_{60}} * \frac{\sum C^+_{60-2n}}{(\sum C^+_{60-2n})_{max}} = \frac{A}{B} * \frac{A}{A_{max}} \tag{6.1}$$

The optimum was defined in this way because it was found earlier that a strong fragmentation yield resulted from the maximum intensity (shortest pulse), which

causes difficulties for an optimization program to properly search parameter space. The regions A and B are graphically shown in Fig. 6.1.

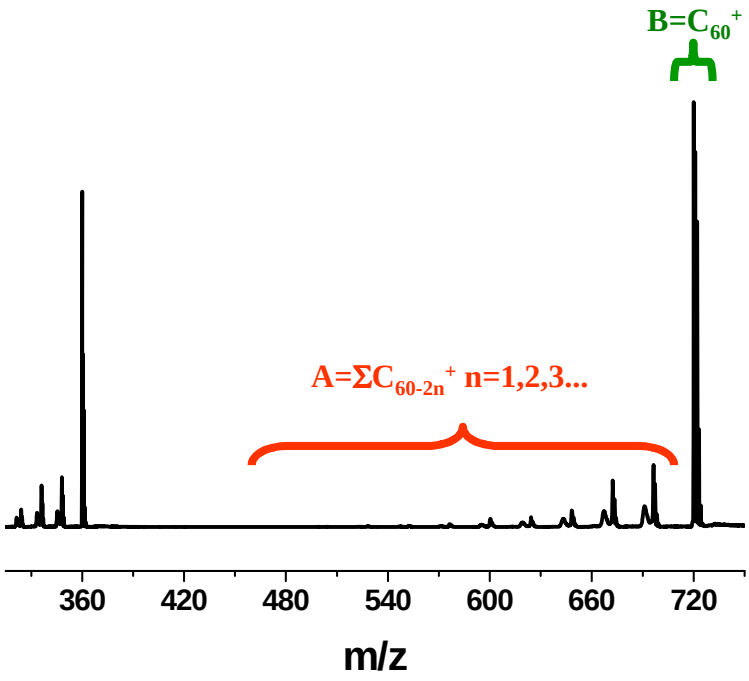

Figure 6.1: *The two regions of a mass spectrum used for the optimization of* C^+_{60-2n} *. A is the region* C^+_{60-2n} *and B is the region* C^+_{60} *. The fitness function is defined as F = (A/B)*(A/*A_{max}*.)*

The employment of the evolutionary program has been described in the experimental chapter. Since the optimization landscape is very complex, with many local minima and maxima, a particular optimization of fragmentation was performed more than 20 times to obtain a feeling for the important features of the resultant pulse.

6.2 Experimental Results

6.2.1 Optimization of C^+_{60-2n}

Fig. 6.2a. shows the progression of an optimization experiment with an evolutionary algorithm. The laser energy was 250 μJ per pulse[1], and the bandwidth limited pulse duration was 30 fs at 790 nm central wavelength. The optimization shown here was run without any parameterization, i.e., the optimization was random. The only limitation was that the pixels were grouped by 4 to reduce the solution space.

For each generation, the ratio of the best individual pattern, the average individual pattern, and the worst individual pattern was recorded. The best pattern is shown with squares, with a thick solid line used to guide the eye. The ratio is seen to improve up to a ratio of 3 after 60 generations. The optimization was aborted after 70 generations since a threshold had been reached. While the ratio of the best maps the progress of the optimal pulse, the median and worst (triangles and circles, respectively) give insight into the diversity of the population. In Fig. 6.2, a wide diversity is observed, which implies either that the pulse forms of different individuals are significantly different, or that slight variations in the pattern cause large signal differences. For C_{60} , the reason for the diversity is expected to be the former, which is controlled by the mutation parameter. A high mutation probability and large changes in the genes will cause a large diversity. The straight horizontal line displays the level of the bandwidth limited pulse. The best pulse shows an increase of a factor of three over the bandwidth limited pulse. In Fig. 6.2b., the cross correlation of the optimal pulse is shown after N generations. In the top panel, the beginning laser pulse is plotted.

The characterization of the resulting optimal pulse shape for the optimization progression of Fig. 6.2 is shown in Fig. 6.3. The left side of Fig.6.2 shows the temporal pulse form measured by SHG background free cross correlation, and the right side shows the complementary SHG-XFROG. In both graphs, the leading edge of the pulse, i.e., the part which interacts with the C_{60} molecule first, is on the right. The resultant pulse shows a strong peak leading three weaker peaks (signal below 0.25 V is regarded as insignificant). The spacing of these maxima is about 250 fs $\pm$ 50 fs, with the entire spread of the electric field about 1 ps. Discussion about the interpretation will be presented later.

[1]This corresponds to an estimated maximum intensity of $5*10^{13}$ W/cm^2 using the bandwidth limited pulse duration of 30 fs.

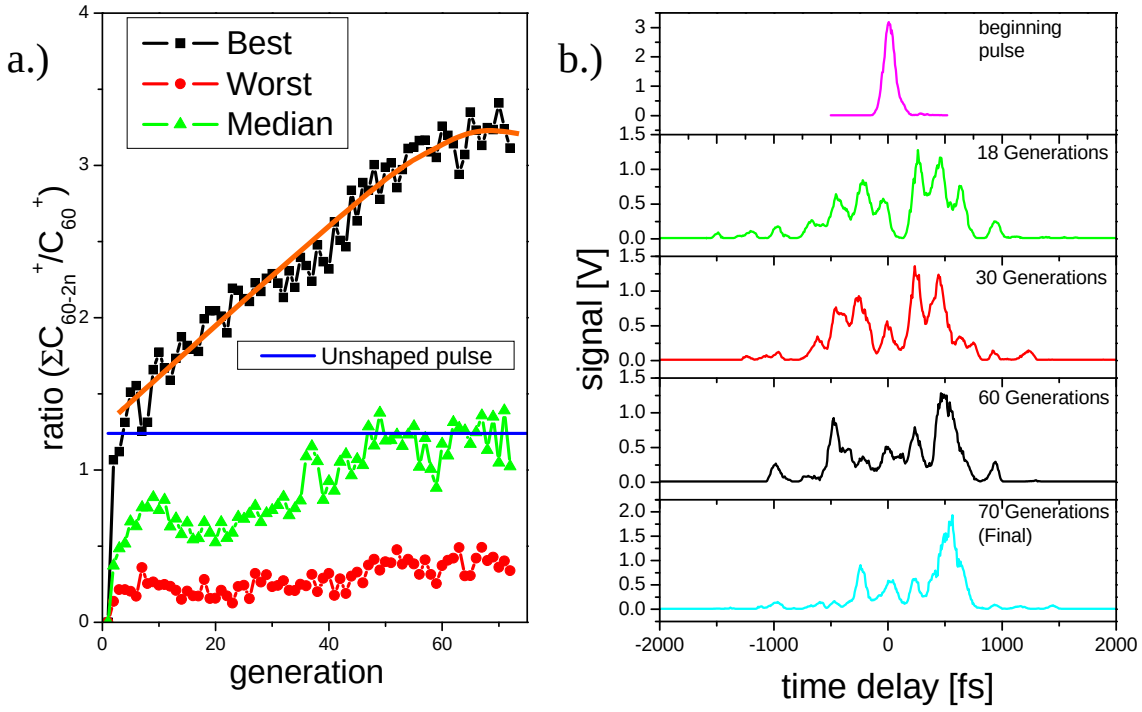

Figure 6.2: *a.)Progression of optimization of C^+_{60-2n} performed with a laser pulse energy of 250 μJ, with a central wavelength of 800 nm, and a bandwidth limited pulse duration of 30 fs. b.) plots the cross correlation of the optimal pulse at several points along the optimization progression. The top panel is the beginning pulse.*

Although the output pulse forms change slightly from optimization run to optimization run, the pulse presented in Fig. 6.3 is representative of the majority (80-90%) of optimal pulses resulting from this optimization. The largest difference occurs in the spacing and amplitude of the weaker peaks trailing the stronger peak.

6.2.2 Proof of Optimization

Now that an optimum has been found, several tests must be made to conclude that this is due to optimization and not simply an artefact of the optimization parameter "ratio". Secondly, the importance of the pulse form will be investigated. Finally, the robustness of the optimization pattern and procedure will be considered.

First, it can be clearly seen in a comparison of the optimal mass spectrum and the mass spectrum of a bandwidth limited pulse that an increase in the ratio is due primarily to the increase in yield of the fragments C^+_{60-2n} and not a decrease of C^+_{60}.

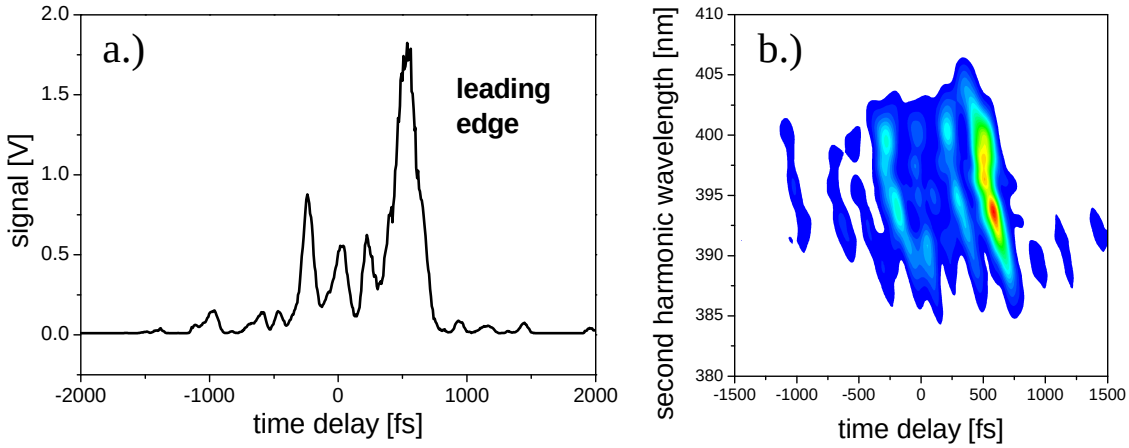

Figure 6.3: *Temporal pulse characterization of the optimal pulse measured with a.) SHG cross-correlation and b.) SHG-XFROG. The laser pulse energy was 250 μJ, with a central wavelength of 790 nm, and a bandwidth limited pulse duration of 30 fs.*

Fig. 6.4a. shows the mass spectrum resulting from a bandwidth limited pulse and Fig. 6.4b. show the resulting mass spectrum from an optimal pulse form. Each plot has been averaged over multiple measurements. Both spectra were recorded with the same energy per pulse, 250 μJ. Indicated on the plots are the integrals over two regions of interest: C^+_{60-2n} and C^+_{60} . The C^+_{60} signal remains similar for both pulses, while the C^+_{60-2n} fragments increase by a factor of 3.01:1.24.[2]

The second point to consider is whether the structure of the shaped pulse is significant or it simply acts like a stretched pulse. This concern arises since a pulse with a pulse duration of 5 ps has been shown to cause more fragmentation than a femtosecond pulse of similar fluence [CHH01]. Fig. 6.5 compares the shaped pulse to several stretched pulses of different durations.

Finally, the robustness of the optimal pulses and optimization program will be considered. A key to optimization, as with any experiment, is a good signal-to-noise ratio. Even if the total change of signal over an optimization run is much larger than the noise, the noise will still affect the optimization as it approaches the threshold and may inhibit finding the optimum. The stability of the ratio of one of the optimal patterns was measured versus real time. The optimum pulse shape (see Fig. 6.3) was selected and repeatedly measured for time scales corresponding to the length of the typical optimization run (>3 hours). Each point represents the ratio of

[2]The ratio changes slightly with varying oven temperatures and/or laser conditions.

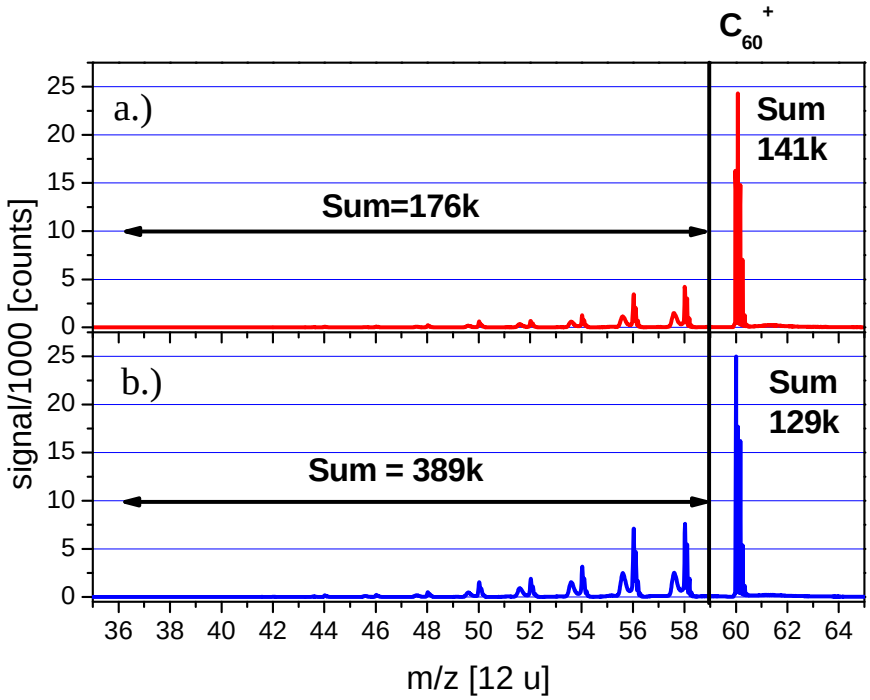

Figure 6.4: *Comparison of mass spectra from an a.) bandwidth limited pulse and an b.) optimal pulse. Each spectrum was recorded with equivalent experimental conditions. The amount of energy per pulse was 250 μJ. The ratio in a.) is 1.24 and the ratio in b.) 3.01.*

heavy fragments to C_{60}^{+} (for this measurement, $A/A_{max} = 1$) summed over 3000 laser shots, which is the same integration time as in the experiments. The mean value is determined from the numerous points, and subsequently the percent difference can be calculated for each point by % Diff $= 100 * (ratio - mean)/mean$. Fig. 6.6 plots the percent difference versus real time. The temperature and laser energy were monitored several times during the experiment and are displayed in Table 6.2.2.

Several features are observed in the resulting curve. There is a broad oscillation, which varies over the time period of hours. This can be attributed to a slow temperature variations of the oven. As was shown in Chapter 2, even slight changes in temperature of 3 degrees can affect the signal amount by approximately 10%. In Fig. 6.6, the slow variation of the ratio changes around 5-10%, thus the ratio is also very sensitive to the oven temperature. Superimposed on this dynamic is a faster oscillation with a 20 minute period. These oscillations most probably arise from laser instability, which can derive from a host of problems (e.g., room temperature or cool-

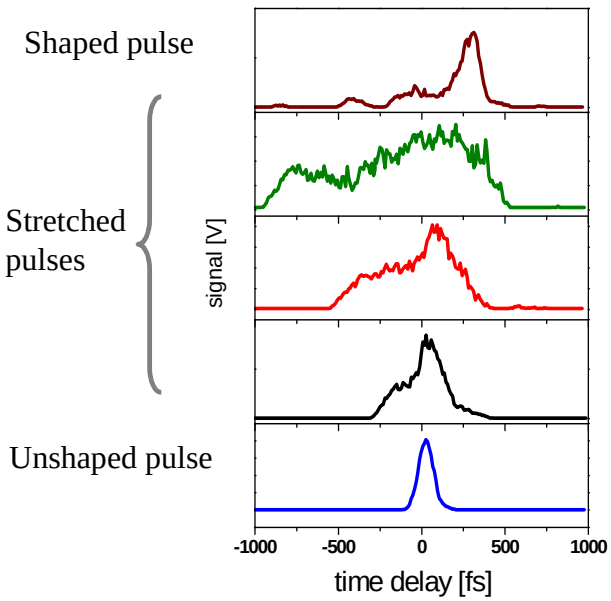

Ratio	Pulse Duration
2.26	-----
0.76	~1000 fs
0.81	~700 fs
0.95	~400 fs
0.98	105 fs

Figure 6.5: *Comparison of the ratio from an optimal pulse to the ratio of several stretched pulses. The energy per pulse was held constant at 250 μJ. The optimal pulse ratio is seen to be significantly higher than the stretched pulses.*

ing water temperature). The finest oscillations are the variation of the ratio on an collection time to collection time basis. This can arise from air fluctuations.

The standard deviation of the ratio over the 200 minute measurement is $\pm = 6.9$ %, and the maximum deviation from the mean value approaches 25%. These values are significantly smaller than the percent difference between optimum and bandwidth limited pulse duration (~300% for similar experimental parameters), allowing for the evolutionary algorithm to converge to a value significantly above the initial signal.

Two parameters can be experimentally varied to determine their importance on the yield: the oven temperature and the laser pulse energy (fluence). In Fig. 6.7, the mass spectrum is measured for an optimal pulse shape at several different laser fluences and the spectra are accumulated over 30000 laser shots. The oven temperature remained constant at 501°C ± 1°C. The ratio of $\sum C^+_{60-2n}$ / C^+_{60} is found to increase linearly with laser energy in a log-log plot over the measured region. A fluence dependence for other optimal laser pulses has not been made, but is expected to produce similar results.

The second parameter, the oven temperature, was measured at a constant pulse

Table 6.1: *Measured temperature and pulse energy for the signal stability measurements of Fig. 6.6. The measured temperature and laser stability is within 2%.*

Time since start (min)	Temperature (°C)	Laser Energy (μJ)
0	502-3	240
74	502	236
101	501	240
139	502	240
171	502	238
207	501	236

energy for several different optimal pulses. Five different temperatures were chosen which cover the entire range of temperatures used in the optimization experiments and is shown in Fig. 6.8. Each point was measured twice and averaged. A constant pulse energy of 245 μJ was used. Six optimal pulses and the bandwidth limited pulse were obtained on different days and are compared. Each trace has an exponential increase over the temperature range. One also notices that the order of optimal pulses does not change, i.e., the absolute optimum remains higher in ratio than the second, and that remains higher than the third, etc. This is furthermore seen to remain true day to day, despite different laser and oven conditions. In Fig. 6.9, a comparison of different patterns acquired after each optimization run is shown. It is clear that the ratio of the optimal pulses is always significantly greater than that of the bandwidth limited pulse. Secondly, it is seen that the patterns remain ordered with respect to each other.

6.3 Discussion

The resultant temporal pulse form plotted in Fig. 6.3 clearly enhances the fragmentation as seen in Fig. 6.4. Further tests have shown that it is robust against oven temperature (Fig. 6.8) and fluence (Fig. 6.7), and is also seen to be superior to a

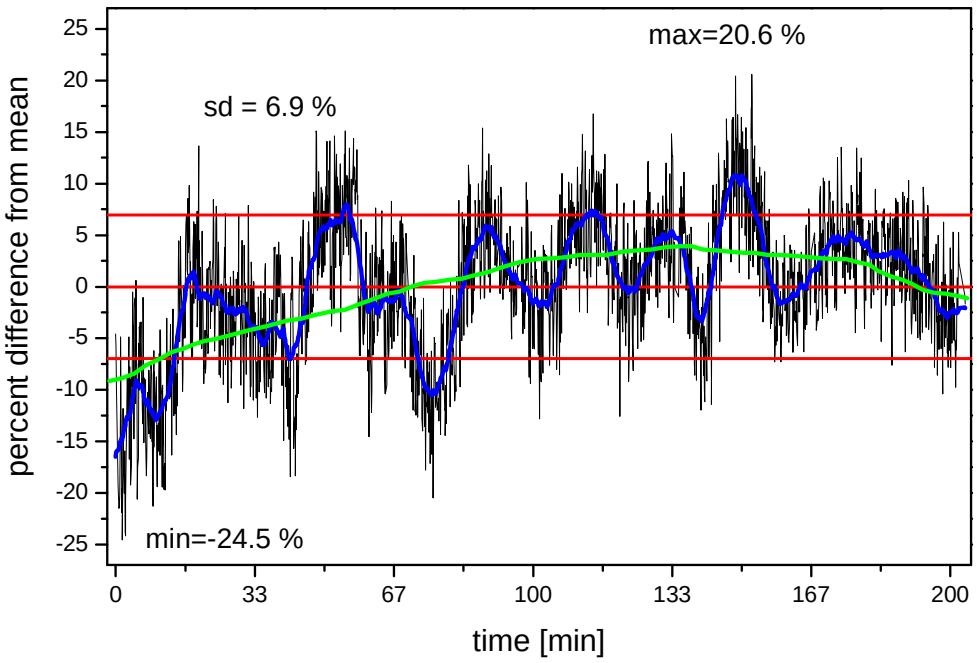

Figure 6.6: *A measurement of the signal stability over the time duration of a typical optimization experiment. The ratio of an optimal pulse was continuously recorded (in 3s intervals) in real time. The laser energy at the beginning was 248 μJ per pulse.*

stretched pulse of equal fluence and similar duration. (Fig. 6.5).

Although only one particular optimal pulse form is shown, the primary feature observed is exemplary of the majority of optimal pulses, namely the strong amplitude followed by a succession of weaker maxima. The spacing of trailing peaks in Fig. 6.3 do not correspond to vibrational frequencies in the ground state. The spacing of 200-300 fs, however, is consistent with the coupling time between electronic and vibrational degrees of freedom. This can be considered to enhance the fragmentation in the following scenario: as the energy flows into the vibrational degrees of freedom from the electronic degrees of freedom, more excitation of the electronic system would be possible without causing further ionization. It should be noted that the exact spacing, amplitude, and number of the trailing maxima are not reproducible, indicating that these parameters are of less importance to the optimum formation of fragments, as long as additional energy is input into the system at some later time. Further experiments need to be performed to understand the nature of the trailing peaks and their importance to fragmentation.

The optimal pulse form is in agreement with pump-probe spectroscopy, where an

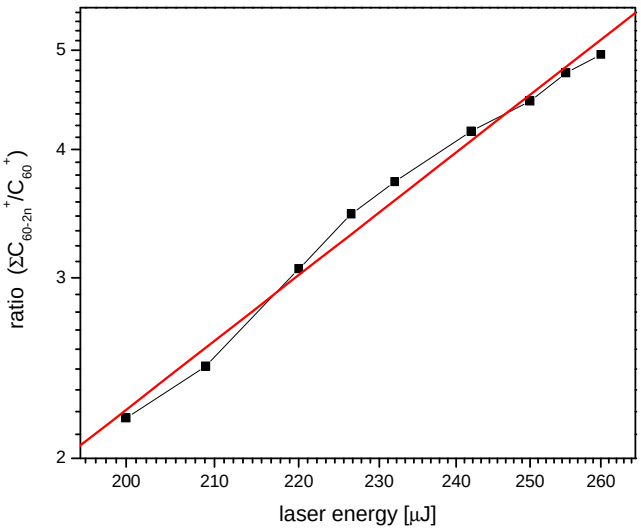

Figure 6.7: *Laser pulse energy influence on the yield from an optimal pulse. The temperature was held constant during the experiment at 501° C.*

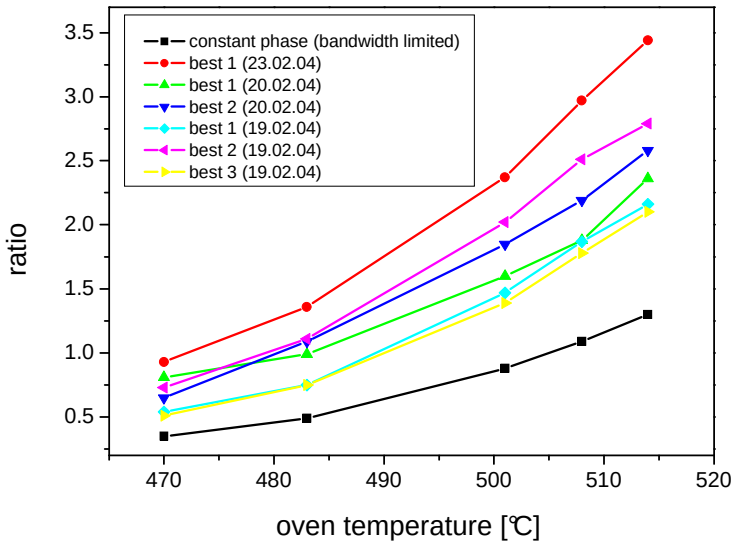

Figure 6.8: *Temperature influence on the ratio at constant laser pulse energy, 245 µJ.*

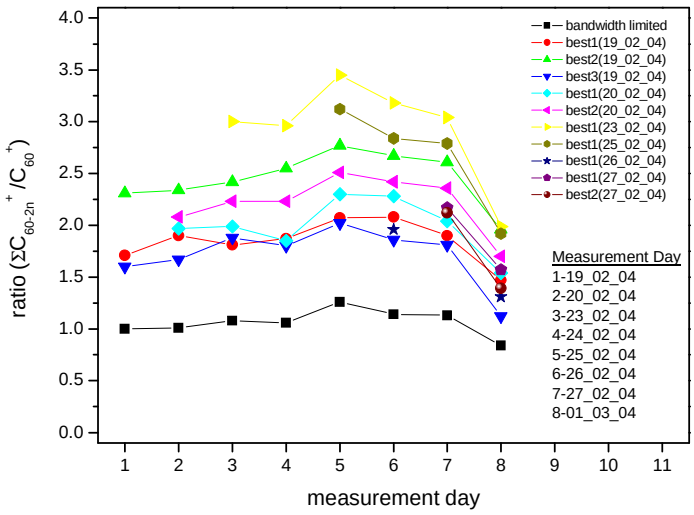

Figure 6.9: *Comparison of optimal patterns on different days. Although the oven temperature and laser energy slightly vary, the order of the pulses remains the same.*

enhancement of fragmentation of the species C_{60-2n}^{+} is observed when a stronger (or blue) pulse leads a weaker pulse (see Chapter 5), which indicates that the time position of the strong pulse is important. The strong leading amplitude can be interpreted to be exciting an intermediate state, from which the absorption of further energy is enhanced, since increased fragmentation is expected to arise from higher internal energies.

The most likely explanation of the optimal temporal pulse shape is that the leading edge directly ionizes the C_{60} molecule through multi-photon ionization. Once the ionic state is reached, the C_{60}^{+} molecules fragment readily when additional energy is absorbed [HAA00]. The optimal energy input is achieved by spacing the energy input so that the energy absorbed from previous pulses can relax from the electronic to the vibrational degrees of freedom.

However, this is only a hypothesis, which needs to be tested. From the present measurements, it is not certain which mechanism leads to an increase in the amount of fragmentation of C_{60-2n}^{+}. Interpretation is further hindered since the intermediate states are unknown. The interpretation of the optimal pulse lies heavily on which charge state the dynamics proceed through. Also, it is not possible to know with certainty if a relaxation from an intermediate state to a second intermediate state is helpful for the optimization procedure.

Recollision of photoelectrons is not expected to be important for the singly charged

fragments [BCR04]. Predicted recollision energies for singly charged species are about 13 eV result in a relatively small absolute cross-section for the electron-impact induced fragmentation of C_2 [HAA00].

6.4 Summary and Outlook

The application of an evolutionary algorithm for enhancement of fragmentation of C_{60}^+ has been successfully employed in this work. The resultant optimal pulse is characterized by a strong leading peak, followed by several weaker peaks. The first, qualitative interpretation to explain the pulse form is that the strong leading peak removes an electron and is followed by further absorption of energy which fragments the C_{60}^+ molecule. This is in agreement with one-color pump-probe measurements where the C_{60}^+ yield is enhanced when the stronger pulse is leading. More experimental work needs to be done to better understand the pulse form.

One particularly important issue to address is the time of ionization. Does the molecule ionize within the leading edge of the shaped pulse? Or does the trailing part remove the electron? The interpretation will depend on whether most of the excitation is in the neutral or ionic system.

For the C_{60} molecule, where no obvious direct dissociation pathways exist, it appears that fragmentation is solely a question of the amount of internal energy absorbed. This holds true particularly for the heavy fragments of fullerenes.

Selective optimization of one particular fragment, for example C_{50}^+, does not result in a dominant C_{50}^+ peak. The statistical nature of the fragmentation of fullerenes does not allow for a clean fragmentation for optimization of one particular fragment. The dominant fragmentation channel, even for femtosecond laser irradiation for the heavy fragments(see Chapter 5), is sequential C_2 loss. The statistical nature is enhanced due to the experimental distribution of the number of photons actually absorbed.

With a little success, the floodgates for optimization ideas open. Many optimizations come to mind in the context of understanding laser interaction with C_{60}. For example, from Chapter 4, optimization of Rydberg states might yield hints concerning their formation, which in turn yields information on the absorption of energy. From Chapter 5, the small fragments would be interesting to optimize because of their time dependence on short (< 10 ps) time scales. Furthermore, optimization of higher charge states, either the fragments, C_{60-2n}^{z+}, or mother ions, C_{60}^{z+}, may yield

interesting information about the interplay between fragmentation or further ionization. For example, as Bhardwaj, et al. show [BCR04], the ratio of fragments $C_{60-2n}^{(z-1)+}$ to C_{60}^{z+} is dependent on the ellipticity of the laser polarization due to recollision of an emitted electron with the ion.

It is important to remember that while an optimization may or may not work, the understanding of why is crucial, and for large systems this is a very challenging task. The experimental work presented here will hopefully entice theoreticians to consider the interaction of C_{60} with optimal pulses.